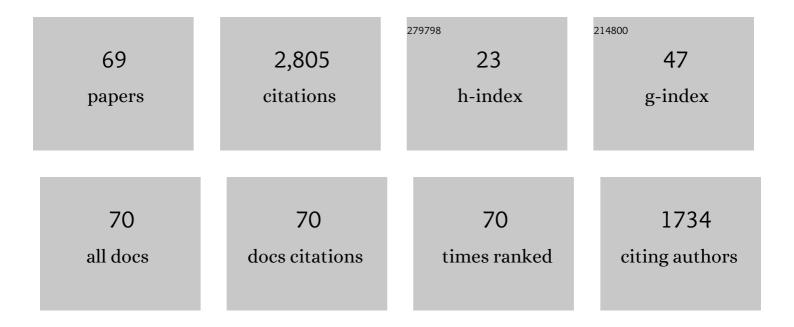
## Sun Lin

## List of Publications by Year in descending order

Source: https://exaly.com/author-pdf/2206819/publications.pdf Version: 2024-02-01



STIN LIN

#	Article	IF	CITATIONS
1	Extending the EOS Long-Term PM <sub>2.5</sub> Data Records Since 2013 in China: Application to the VIIRS Deep Blue Aerosol Products. IEEE Transactions on Geoscience and Remote Sensing, 2022, 60, 1-12.	6.3	7
2	Satellite Aerosol Retrieval Using Scene Simulation and Deep Belief Network. IEEE Transactions on Geoscience and Remote Sensing, 2022, 60, 1-16.	6.3	3
3	GF-4 Satellite Fire Detection With an Improved Contextual Algorithm. IEEE Journal of Selected Topics in Applied Earth Observations and Remote Sensing, 2022, 15, 163-172.	4.9	1
4	A Novel Method for Hyperspectral Mineral Mapping Based on Clustering-Matching and Nonnegative Matrix Factorization. Remote Sensing, 2022, 14, 1042.	4.0	7
5	Estimation of Aerosol Optical Depth at 30 m Resolution Using Landsat Imagery and Machine Learning. Remote Sensing, 2022, 14, 1053.	4.0	6
6	Global Cross-Sensor Transformation Functions for Landsat-8 and Sentinel-2 Top of Atmosphere and Surface Reflectance Products Within Google Earth Engine. IEEE Transactions on Geoscience and Remote Sensing, 2022, 60, 1-9.	6.3	2
7	Ground-Level NO <sub>2</sub> Surveillance from Space Across China for High Resolution Using Interpretable Spatiotemporally Weighted Artificial Intelligence. Environmental Science & Technology, 2022, 56, 9988-9998.	10.0	90
8	Temperature-Based and Radiance-Based Validation of the Collection 6 MYD11 and MYD21 Land Surface Temperature Products Over Barren Surfaces in Northwestern China. IEEE Transactions on Geoscience and Remote Sensing, 2021, 59, 1794-1807.	6.3	56
9	MODIS aerosol optical depth retrieval based on random forest approach. Remote Sensing Letters, 2021, 12, 179-189.	1.4	8
10	Reconstructing 1-km-resolution high-quality PM2.5 data records from 2000 to 2018 in China: spatiotemporal variations and policy implications. Remote Sensing of Environment, 2021, 252, 112136.	11.0	429
11	Inferring Near-Surface PM2.5 Concentrations from the VIIRS Deep Blue Aerosol Product in China: A Spatiotemporally Weighted Random Forest Model. Remote Sensing, 2021, 13, 505.	4.0	12
12	The ChinaHighPM10 dataset: generation, validation, and spatiotemporal variations from 2015 to 2019 across China. Environment International, 2021, 146, 106290.	10.0	168
13	Himawari-8-derived diurnal variations in ground-level PM <sub>2.5</sub> pollution across China using the fast space-time Light Gradient Boosting Machine (LightGBM). Atmospheric Chemistry and Physics, 2021, 21, 7863-7880.	4.9	86
14	Assessing the Self-Recovery Ability of Maize after Lodging Using UAV-LiDAR Data. Remote Sensing, 2021, 13, 2270.	4.0	10
15	Cloud Detection Algorithm for Multi-Satellite Remote Sensing Imagery Based on a Spectral Library and 1D Convolutional Neural Network. Remote Sensing, 2021, 13, 3319.	4.0	13
16	Leaf area index remote sensing based on Deep Belief Network supported by simulation data. International Journal of Remote Sensing, 2021, 42, 7637-7661.	2.9	4
17	Retrieving High-Resolution Aerosol Optical Depth from GF-4 PMS Imagery in Eastern China. Remote Sensing, 2021, 13, 3752.	4.0	4
18	An Improved DDV Algorithm for the Retrieval of Aerosol Optical Depth From NOAA/AVHRR Data. Journal of the Indian Society of Remote Sensing, 2021, 49, 1141-1152.	2.4	4

Sun Lin

#	Article	IF	CITATIONS
19	Atmospheric Correction of GF-6/WFV Sensor Supported by Modis. , 2021, , .		0
20	Land Surface Temperature Retrieval from Nighttime Mid-Infrared Modis Data Using a Split-Window Algorithm. , 2021, , .		0
21	Analysis of Land Use and Land Cover Changes in Urban Areas Using Remote Sensing: Case of Blantyre City. Discrete Dynamics in Nature and Society, 2021, 2021, 1-17.	0.9	13
22	An Improved Fmask Method for Cloud Detection in GF-6 WFV Based on Spectral-Contextual Information. Remote Sensing, 2021, 13, 4936.	4.0	2
23	Satellite data cloud detection using deep learning supported by hyperspectral data. International Journal of Remote Sensing, 2020, 41, 1349-1371.	2.9	29
24	Improved cloud detection for Landsat 8 images using a combined neural network model. Remote Sensing Letters, 2020, 11, 274-282.	1.4	7
25	MODIS Collection 6.1 3Âkm resolution aerosol optical depth product: global evaluation and uncertainty analysis. Atmospheric Environment, 2020, 240, 117768.	4.1	44
26	MODIS Aerosol Optical Depth Inversion Over Urban Areas Supported by BRDF/Albedo Products. Journal of the Indian Society of Remote Sensing, 2020, 48, 1345-1354.	2.4	1
27	An Operational Split-Window Algorithm for Retrieving Land Surface Temperature from Geostationary Satellite Data: A Case Study on Himawari-8 AHI Data. Remote Sensing, 2020, 12, 2613.	4.0	14
28	Retrieval and Validation of AOD from Himawari-8 Data over Bohai Rim Region, China. Remote Sensing, 2020, 12, 3425.	4.0	4
29	Improved 1 km resolution PM <sub>2.5</sub> estimates across China using enhanced space–time extremely randomized trees. Atmospheric Chemistry and Physics, 2020, 20, 3273-3289.	4.9	321
30	Aerosol Inversion for Landsat 8 Oli Data Using Deep Learning Algorithm. , 2020, , .		0
31	Retrieval of Aerosol Optical Depth (AOD) from the Landsat8 Oli Observations Over Beijing. , 2020, , .		1
32	Enhanced Aerosol Estimations From Suomi-NPP VIIRS Images Over Heterogeneous Surfaces. IEEE Transactions on Geoscience and Remote Sensing, 2019, 57, 9534-9543.	6.3	16
33	Comparison of the MuSyQ and MODIS Collection 6 Land Surface Temperature Products Over Barren Surfaces in the Heihe River Basin, China. IEEE Transactions on Geoscience and Remote Sensing, 2019, 57, 8081-8094.	6.3	35
34	Estimating 1-km-resolution PM2.5 concentrations across China using the space-time random forest approach. Remote Sensing of Environment, 2019, 231, 111221.	11.0	340
35	Satellite-Derived 1-km-Resolution PM <sub>1</sub> Concentrations from 2014 to 2018 across China. Environmental Science & Technology, 2019, 53, 13265-13274.	10.0	195
36	Evaluation and uncertainty estimate of next-generation geostationary meteorological Himawari-8/AHI aerosol products. Science of the Total Environment, 2019, 692, 879-891.	8.0	46

Sun Lin

#	Article	IF	CITATIONS
37	Intercomparison in spatial distributions and temporal trends derived from multi-source satellite aerosol products. Atmospheric Chemistry and Physics, 2019, 19, 7183-7207.	4.9	82
38	Estimating PM2.5 Concentrations Based on MODIS AOD and NAQPMS Data over Beijing–Tianjin–Hebei. Sensors, 2019, 19, 1207.	3.8	32
39	Improved Aerosol Retrievals Over Complex Regions Using NPP Visible Infrared Imaging Radiometer Suite Observations. Earth and Space Science, 2019, 6, 629-645.	2.6	20
40	Mineral Mapping with Hyperspectral Image Based on an Improved K-Means Clustering Algorithm. , 2019, , .		11
41	MODIS Aerosol Inversion Under Complex Background Conditions Supported By BRDF/ALBEDO Products. , 2019, , .		0
42	High Temporal Resolution Land Surface Temperature Retrieval from Global Geostationary Satellite Data. , 2019, , .		0
43	MODIS Collection 6.1 aerosol optical depth products over land and ocean: validation and comparison. Atmospheric Environment, 2019, 201, 428-440.	4.1	209
44	Monitoring Maize Lodging Grades via Unmanned Aerial Vehicle Multispectral Image. Plant Phenomics, 2019, 2019, 5704154.	5.9	28
45	Verification, improvement and application of aerosol optical depths in China Part 1: Inter-comparison of NPP-VIIRS and Aqua-MODIS. Atmospheric Environment, 2018, 175, 221-233.	4.1	72
46	A Temperature and Emissivity Separation Algortihm for Chinese Gaofen-5 Satelltie Data. , 2018, , .		2
47	An Improved Highâ€Spatialâ€Resolution Aerosol Retrieval Algorithm for MODIS Images Over Land. Journal of Geophysical Research D: Atmospheres, 2018, 123, 12,291.	3.3	42
48	<italic>A Priori</italic> Surface Reflectance-Based Cloud Shadow Detection Algorithm for Landsat 8 OLI. IEEE Geoscience and Remote Sensing Letters, 2018, 15, 1610-1614.	3.1	6
49	Retrieval of Aerosol Optical Depth in the Arid or Semiarid Region of Northern Xinjiang, China. Remote Sensing, 2018, 10, 197.	4.0	23
50	A Simple and Universal Aerosol Retrieval Algorithm for Landsat Series Images Over Complex Surfaces. Journal of Geophysical Research D: Atmospheres, 2017, 122, 13,338.	3.3	44
51	Detection and validation of dust storm from NPP VIIRS. , 2017, , .		0
52	Validation and Accuracy Analysis of Global MODIS Aerosol Products over Land. Atmosphere, 2017, 8, 155.	2.3	21
53	A comparison of the cloud detection results between the UDTCDA mask and MOD35 cloud products. , 2017, , .		1
54	Retrieval of Aerosol Optical Depth over Arid Areas from MODIS Data. Atmosphere, 2016, 7, 134.	2.3	10

~		
	11NI	LIN
ິ	un	

#	Article	IF	CITATIONS
55	Aerosol Optical Depth Retrieval over Bright Areas Using Landsat 8 OLI Images. Remote Sensing, 2016, 8, 23.	4.0	89
56	Dynamic threshold cloud detection algorithms for MODIS and Landsat 8 data. , 2016, , .		6
57	A high-resolution global dataset of aerosol optical depth over land from MODIS data. , 2016, , .		2
58	Retrieving land surface temperature from Landsat 8 TIRS data using RTTOV and ASTER GED. , 2016, , .		7
59	A Universal Dynamic Threshold Cloud Detection Algorithm (UDTCDA) supported by a prior surface reflectance database. Journal of Geophysical Research D: Atmospheres, 2016, 121, 7172-7196.	3.3	70
60	Land surface temperature retrieval from HJ-1B IRS supported by MODIS. , 2013, , .		1
61	Remote Sensing Technology's Applied Research and Development Direction in Land-Use and Land-Cover Change (LUCC). , 2012, , .		1
62	Land surface emissivity retrieval from HJ-1B satellite data using a combined method. , 2011, , .		0
63	Effects of dust from the west of China on the particulate pollution in mid-eastern cities. , 2011, , .		0
64	Extraction of Land Cover Information in East China based on MODIS data. , 2011, , .		0
65	Retrieving BRDF of desert using time series of MODIS imagery. , 2011, , .		0
66	Extraction of Normalized Difference vegetation index from HJ-1A/B CCD. , 2011, , .		0
67	Aerosol optical depth retrieval by HJ-1/CCD supported by MODIS surface reflectance data. Science China Earth Sciences, 2010, 53, 74-80.	5.2	44
68	Extracting impervious surface distribution and changing information of Shenyang. , 2009, , .		1
69	Retrieval of aerosol optical thickness from HJ-1A/B images using structure function method. , 2009, , .		2